

# Study of the ${}^2\text{H}(p, \gamma){}^3\text{He}$ reaction in the Big Bang Nucleosynthesis energy range at LUNA

Viviana Mossa (for the LUNA collaboration)<sup>1</sup>

<sup>1</sup> *Università degli Studi di Bari and INFN sez. Bari*

**Abstract.** Deuterium is the first nucleus produced in the Universe, whose accumulation marks the beginning of the so called Big Bang Nucleosynthesis (BBN). Its primordial abundance is very sensitive to some cosmological parameters like the baryon density and the number of the neutrino families. Presently the main obstacle to an accurate theoretical deuterium abundance evaluation is due to the poor knowledge of the  ${}^2\text{H}(p, \gamma){}^3\text{He}$  cross section at BBN energies. The aim of the present work is to describe the experimental approach proposed by the LUNA collaboration, whose goal is to measure, with unprecedented precision, the total and the differential cross section of the reaction in the  $30 < E_{c.m.}[keV] < 300$  energy range.

## 1 Introduction

The Big Bang Nucleosynthesis describes the production of light nuclides in the first minutes of cosmic time through the reaction chain shown in figure 1. The nucleosynthesis network begins with the formation of deuterium in the process  $p(n, \gamma){}^2\text{H}$ . Nearly all the free neutrons end up bound in the most stable light element  ${}^4\text{He}$ , while  ${}^2\text{H}$ ,  ${}^3\text{He}$ ,  ${}^7\text{Li}$  and  ${}^6\text{Li}$  nuclei form in residual quantities. The synthesis of heavier nuclei is hindered by the absence of stable nuclei with  $A = 8$ .

The primordial abundance of light isotopes depends on the competition between the expansion rate of the Universe and the yields of the reactions shown in figure 1. In the standard cosmology the expansion rate of the Universe is governed by the Friedmann equation  $H^2 = \frac{8\pi}{3}G\rho$ , where  $H$  is the Hubble parameter,  $G$  the gravitational constant and  $\rho$  the energy density, dominated, in the early Universe, by the “radiation”, namely any massless or extremely relativistic particle. Being photons and neutrinos the only known relativistic particles at the BBN epoch, the radiation density can be expressed as  $\rho = \rho_\gamma \left[ 1 + \frac{7}{8} \left( \frac{4}{11} \right)^{4/3} N_{eff} \right]$ , where  $\rho_\gamma$  is the photon density and  $N_{eff}$  the contribution of other relativistic species ( $N_{eff} = 3.046$  if only the three known neutrino families are taken into account). Consequently the primordial abundance of light isotopes depends on the baryon density  $\Omega_b$ , usually expressed normalized to the baryon-to-photon ratio  $\eta$  and on the number of neutrino families or any other relativistic species  $N_{eff}$ . BBN theory can thus provide a powerful tool to constrain these cosmological parameters.

## 2 Physics motivation for a new ${}^2\text{H}(p, \gamma){}^3\text{He}$ measurement at BBN energies

Recent observations of Cosmic Microwave Background (CMB) anisotropies by the Planck satellite [1] constrain the cosmological parameters with such a high level of accuracy that the primordial deu-

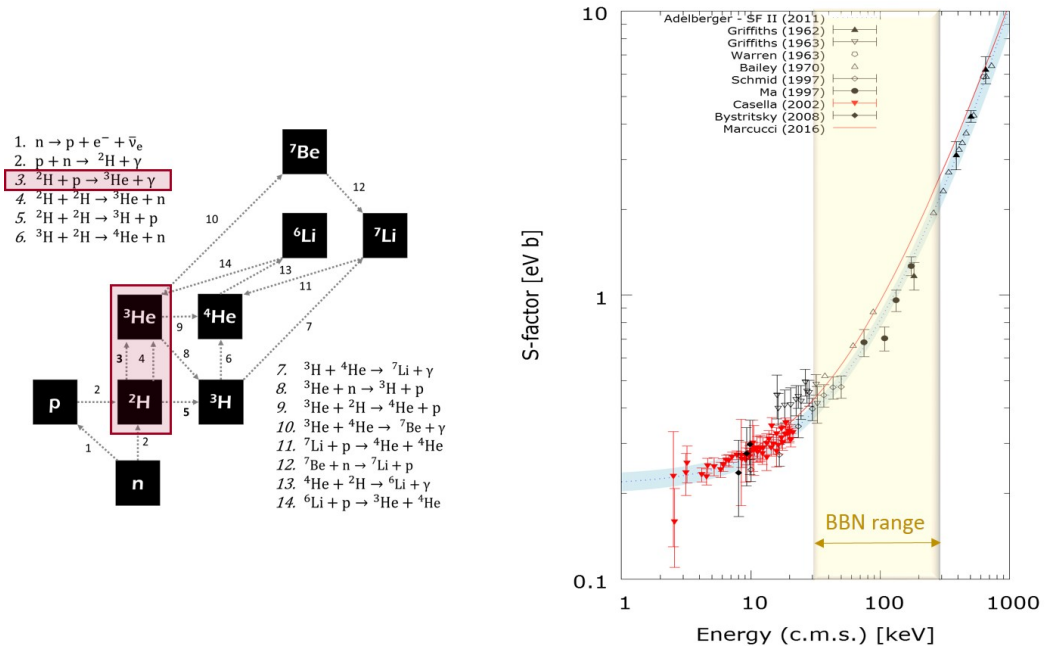


**Figure 1.** On the left the leading processes of Big Bang Nucleosynthesis. On the right  ${}^2\text{H}(p, \gamma){}^3\text{He}$  S-factor as a function of center of mass energy. The blue band represents the 68% lower and upper bound of the adopted quadratic best fit of Adelberger et al.

terium abundance can be inferred with remarkable precision. In particular, assuming the Planck baryonic density in a standard cosmological scenario and using the standard BBN dynamics, it is possible to compute the abundance of primordial deuterium  $(D/H)_{BBN} = (2.65 \pm 0.07) \times 10^{-5}$  [2].

The result of BBN theory has to be compared with the direct observations of Damped Lyman-Alpha (DLA) systems at high redshift according to which the deuterium abundance is smaller than the indirect and model-dependent cosmological determination with a higher accuracy  $(D/H)_{obs} = (2.547 \pm 0.033) \times 10^{-5}$  [3].

These two deuterium abundance determinations, while broadly consistent, are off by about one standard deviation. This is mainly due to the uncertainty with which the cross sections of the nuclear processes involved in deuterium creation and destruction are known. Presently the main source of uncertainty is the radiative capture process  ${}^2\text{H}(p, \gamma){}^3\text{He}$  converting deuterium into helium, because of the poor knowledge of its S-factor at BBN energies. In fact, as shown in figure 1 (right side), while the low energy limit of this reaction cross section is well known thanks to the data coming from the LUNA measurement performed within the solar Gamow peak [4], in the BBN energy range only a single data set is currently available with a systematic error of 9%.

The astrophysical S-factor of the  ${}^2\text{H}(p, \gamma){}^3\text{He}$  reaction is of high interest also for theoretical nuclear physics, in particular for what concern “ab-initio” calculations [5], providing an accurate prediction for the total and the differential cross section at low energies. Conversely, as highlighted by the plot in figure 1, in the BBN energy range, the theoretical result is systematically higher than data [6] by 20-30%. This huge difference between theory and data makes the situation undefined, letting some author to adopt the theoretical curve and others the S-factor value obtained from the direct measurements.

### 3 The ${}^2\text{H}(p, \gamma){}^3\text{He}$ reaction at BBN energies at LUNA

The measurement of the  ${}^2\text{H}(p, \gamma){}^3\text{He}$  cross section is ongoing at the Laboratory for Underground Nuclear Astrophysics (LUNA) taking advantage of the low background of the underground Gran Sasso Laboratories and of the experience accumulated in more than twenty years of scientific activity on precision measurements.

The new  ${}^2\text{H}(p, \gamma){}^3\text{He}$  measurement at LUNA will exploit a 400 kV electrostatic accelerator [7] able to provide intense current of proton up to  $500 \mu\text{A}$  with a precise absolute energy ( $\pm 0.3 \text{ keV}$ ), low spread ( $< 0.1 \text{ keV}$ ) and long-term stability ( $5 \text{ eV/h}$ ) and a windowless deuterium gas target, consisting of three-stage pumping system able to increase the gas pressure from the accelerator high vacuum to the mbar level in the target chamber. Since no real window is present, the energy degradation of the proton beam is negligible and the final ion energy is precisely determined. The beam current is measured by a constant-gradient calorimeter characterized by two sides, a hot one heated to  $70^\circ\text{C}$  by thermoresistors and a cold one cooled to  $-5^\circ\text{C}$  by a refrigerating system [8]. When the ion beam hits the hot side, it contributes to its heating and reduces correspondingly the electric power needed to keep the temperature gradient constant. The current impinging on the target is thus related to the power difference between beam-on and beam-off conditions.

The experimental procedure consists of two main phases characterized by two different set-ups. The former foresees a deuterium gas target 10 cm long at 0.3 mbar of pressure and a cylindrical BGO detector having a length of 28 cm with a radial thickness of 7 cm. The crystal is optically divided into six sectors, each covering an azimuthal angle of 60 degrees and the chamber and the calorimeter are hosted inside the BGO hole. Thanks to the high detection efficiency (about 60%) in the range of interest for the  ${}^2\text{H}(p, \gamma){}^3\text{He}$  reaction (5.5 MeV), this set-up will provide a cross section measurement down to very low energies. The efficiency calibration can be obtained at a few per cent level using Monte Carlo simulations of the set-up, tuned with radioactive sources ( ${}^{137}\text{Cs}$ ,  ${}^{60}\text{Co}$  and  ${}^{88}\text{Y}$ ) at low energies and with the well-known resonant reaction  ${}^{14}\text{N}(p, \gamma){}^{15}\text{O}$  at  $E_r = 259 \text{ keV}$ , emitting  $\gamma$  rays in the p+d energy range. In order to reduce systematic errors, the spatial position of the resonance has been identified inside the chamber using a well collimated NaI detector in close geometry with the target: keeping the scintillator fixed in the measurement position, the proton energy has been increased and decreased in 2-3 keV steps until the achievement of the maximum counting rate corresponding to the resonance peak.

The latter phase, instead, will cover the medium-high energies ( $70 < E_{\text{c.m.}}[\text{keV}] < 260$ ) using a High Purity Germanium detector (HPGe) in a close geometry with the interaction chamber. This set-up allows to study the angular distribution of the emitted  $\gamma$ -rays, exploiting the high energy resolution of the HPGe detector and the Doppler effect affecting the photons emitted along the beam line. Using an extended deuterium gas target (33 cm long) at 0.3 mbar of pressure, in fact, the emitted photons are Doppler broadened and the peak width will be dominated by kinematics. Since the angular distribution of the emitted gammas will determine the peak shape, starting from the  $\gamma$ -ray energy spectrum, it is possible to extract the differential cross section of the process. This measurement requires the detection efficiency to be known with high accuracy along all the target chamber. The procedure adopted for measuring it couples the main HPGe detector (Ge1) to an auxiliary one (Ge2) and exploits the coincidence between two  $\gamma$ -rays emitted in cascade. The main decay channel of the  $E_r = 259 \text{ keV}$  resonance (BR=57.8 %) is particularly useful to determine the germanium efficiency, because it is composed by 2 photons with energy  $E_{\gamma_1} = 1384 \text{ keV}$  (close to the energy of  ${}^{60}\text{Co}$   $\gamma$ -rays) and  $E_{\gamma_2} = 6172 \text{ keV}$  (close to the energy of photons produced by the  ${}^2\text{H}(p, \gamma){}^3\text{He}$  reaction). Whenever the auxiliary counter detects an event  $\gamma_1$ , it enables the other counter that can thus detect the corresponding cascade emitted photon  $\gamma_2$ . The detection efficiency of Ge1 can be evaluated by the ratio between the number of events that has triggered the acquisition and the number of events actually acquired by the

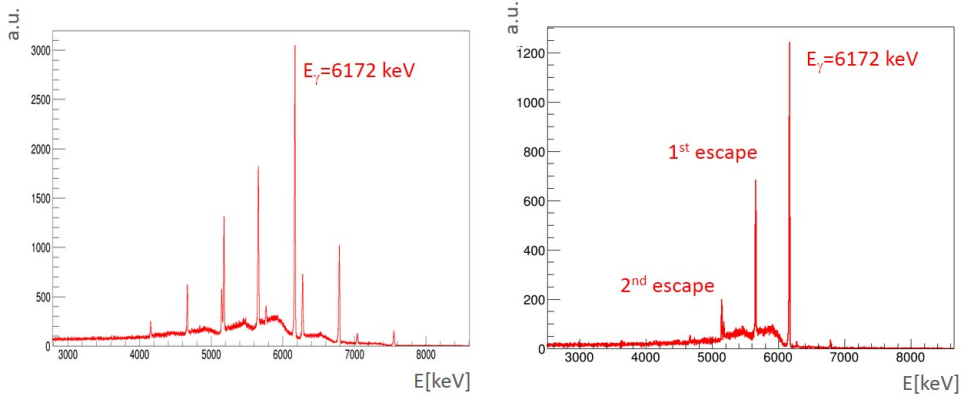


**Figure 2.**  $^{14}\text{N}(p, \gamma)^{15}\text{O}$  resonance spectra: on the left the one acquired in inclusive configuration, on the right the one acquired in coincidence configuration.

detector itself. The effect of the coincidence acquisition is shown in figure 2, where the spectrum of the  $^{14}\text{N}(p, \gamma)^{15}\text{O}$  resonance acquired by Ge1 in inclusive configuration is shown on the left. Selecting the resonance emitted photon at 1.3 MeV with Ge2, the resulting coincidence spectrum of Ge1 (on the right in fig. 2) shows the corresponding cascade photon at 6.1 MeV, with its first and second escape peaks.

## 4 Conclusion

At the moment the BGO phase is completed, while the HPGe data taking and the data analysis of both phases are still on going. The low background and the high quality of the LUNA facility at LNGS will allow the  $^2\text{H}(p, \gamma)^3\text{He}$  cross section to be measured, filling the lack of experimental data in the BBN energy range with a higher precision with respect to the existing one and verifying theoretical nuclear studies. This study is of primary importance also to derive the baryon density of Universe with high accuracy, similar to the one obtained with CMB experiments. Moreover, it allows to constrain the existence of the so called "dark radiation", composed by undiscovered relativistic species permeating the universe, such as sterile neutrinos.

## References

- [1] Plank collaboration, *A& A* **594** A13, 63 (2016)
- [2] Di Valentino E. *et al.*, *Phys. Rev. D* **90**, 023543 (2014)
- [3] Cooke R. *et al.*, *Astrophys. J.* **781**, 31 (2016)
- [4] Casella C. *et al.*, *Nucl. Phys. A* **706**, 203 (2002)
- [5] Marcucci L.E. *et al.*, *Phys. Rev. Lett.* **116**, 10250 (2016)
- [6] Ma L. *et al.*, *Phys. Rev. C* **55**, 2 (1997)
- [7] Formicola A. *et al.*, *Nucl. Inst. Meth. A* **507**, 609(2003)
- [8] Casella C. *et al.*, *Nucl. Inst. Meth. A* **489**, 160 (2002)